

Peter Bayley · Stephen Martin · Peter Browne  
Catherine Royer

## Time-resolved fluorescence anisotropy studies show domain-specific interactions of calmodulin with IQ target sequences of myosin V

Published online: 31 January 2003  
© EBSA 2003

**Abstract** Single cysteine mutants of calmodulin, Cam(S38C) and Cam(N111C), have been specifically labelled with Alexa488 maleimide to study the effects of calcium on the structural dynamics of calmodulin complexed with IQ3, IQ4 and IQ34 target peptide motifs of mouse unconventional myosin-V. Using phase fluorometry, the time-resolved anisotropy shows well-separated global and segmental correlation times. The calcium-sensitive global motion of either calmodulin domain can be independently monitored in domain-specific interactions of either apo- or Ca<sub>4</sub>-calmodulin with IQ3 or IQ4 peptides. C-domain interactions predominate, and apo-N-domain interactions are unexpectedly weak. The 1:1 complex of Ca<sub>4</sub>-calmodulin with IQ34 behaves as a compact globular species. The results demonstrate novel dynamic aspects of calmodulin-IQ interactions relating to the calcium regulation of motility of unconventional myosin.

**Keywords** Calcium-regulated motility · Calmodulin · Fluorescence anisotropy · Rotational correlation · Unconventional myosin

**Abbreviations** *Apo-Cam* Ca-free calmodulin · *Holo-Cam* Ca<sub>4</sub>-calmodulin · *Cam38A*, *Cam111A* calmodulin cysteine mutant labelled at position 38 or 111 with Alexa488 · *ELC*, *RLC* essential and regulatory myosin light chains · *IQ3* AATTIQKYWRMYVRRRYK · *IQ4* IRRAATIVIQSYLRGYLTRNRYR · *IQ34* AATTIQKYWRMYVRRRYKIRRAATIVIQSYLRGY-

LTRNRYR · *sk-*, *sm-MLCK* skeletal, or smooth, muscle myosin light chain kinase

### Introduction

Calmodulin is a small, ubiquitous calcium-binding protein with  $M_r \approx 16$  kD, which functions as a regulatory and Ca-signal transducer in many eukaryotic cells. It is composed of two homologous domains, each domain binding two Ca ions in a pair of EF-hand binding motifs. The two domains are linked by a sequence which appears  $\alpha$ -helical in crystal structure, but which NMR shows to be flexible in solution. The structures of several complexes of Ca<sub>4</sub>-calmodulin with typical (basic, amphipathic  $\alpha$ -helical) target peptides are well established, and collectively emphasize that this flexibility is central to the versatility of calmodulin interaction with a variety of target proteins (Crivici and Ikura 1995).

The myosin family of motor proteins (Cope et al. 1996) have a general structure comprising: (1) the catalytic S1 motor domain, which has an actin-activated ATPase activity, (2) the  $\alpha$ -helical regulatory region of the heavy chain, with attached light chains (e.g., the ELC and RLC of muscle myosin-II) and (3) a specific terminal structure, which, in muscle myosin II, is a long coiled-coil region involved in forming the myosin thick filament. Myosin V is a dimeric myosin with a motor region, regulatory region and coiled-coil tail, to which is attached a globular domain with membrane-binding functions. The motor is processive, taking multiple steps along F-actin before detaching (Mehta et al. 1999; Walker et al. 2000). The regulatory region of members of the myosin family contains copies of a consensus IQ motif, IQxxxRGxxxR (Houdusse et al. 1996), to which light chains bind. In myosin V, calmodulin serves as the light chain, binding to six concatenated IQ sequences which, while homologous, have individual sequence characteristics. Myosin-V isolated from brain contains multiple apo-calmodulin molecules (Collins et al. 1990), and functional recombinant myosin-V requires the

P. Bayley (✉) · S. Martin · P. Browne  
Division of Physical Biochemistry,  
National Institute for Medical Research,  
Mill Hill, London, NW7 1AA, UK  
E-mail: pbayley@nimr.mrc.ac.uk  
Tel.: +44-(0)20 8816 2085

C. Royer  
Centre de Biochimie Structurale,  
UMR5048, CNRS, Montpellier, France

co-expression of calmodulin (Homma et al. 2000). In mouse, it appears that all the myosin-V light chains may be calmodulin (Wang et al. 2000); alternatively (e.g., in chicken), one or more light chains may be species-specific ELC molecules, interacting at IQ1 or IQ2 (De La Cruz et al. 2000), with calmodulin as the light chain for the other IQ sequences. We have therefore studied typical calmodulin interactions with the central target peptides from mouse myosin-V, namely the IQ3, IQ4 and IQ34 sequences (Bayley et al. 2002).

Currently, no detailed structure is available for the complex of apo-calmodulin with an IQ sequence peptide. The structure of the regulatory fragment of scallop myosin (1wdc.pdb) shows the ELC and RLC bound to two IQ-motifs in the helical regulatory segment of myosin II (Houdusse and Cohen 1996). A model (1aji.pdb; Fig. 1) was derived from this structure for the interaction of apo-calmodulin with the IQ sequence of brush border myosin I, BBM-I (Houdusse et al. 1996). The calmodulin is modelled by analogy with scallop ELC, with the apo-C-domain in the “semi-open” conformation and the apo-N-domain in the “closed” form, as seen by NMR (Swindells and Ikura 1996). The orientation of the peptide is reversed compared to that in the complex of  $\text{Ca}_4\text{Cam}$  with the target peptide from skeletal muscle MLCK (1cdl.pdb) (Crivici and Ikura 1995; Houdusse and Cohen 1996). A structure of apo-calmodulin with the IQ12 sequence of myosin V has been reported to conform to the proposed model (1aji.pdb) (Houdusse et al. 2000).

These structures and models indicate that changes in the dynamics of calmodulin are central to the functioning of this versatile regulatory molecule, which has been the subject of previous spectroscopic investigations. The fluorescence anisotropy of the total emission of two intrinsic (C-domain) tyrosine residues of bovine calmodulin has previously been studied using time-domain (Bayley et al. 1988; Török et al. 1992) and frequency-domain measurements (reviewed in Anderson 1991). In the present work, the domain-specific fluores-

cence labelling of recombinantly expressed *Drosophila* calmodulin mutants is used to examine  $\text{Ca}^{2+}$ -dependent differences in the dynamic behaviour of the two domains of intact calmodulin in the interactions with IQ3, IQ4 and the double-length IQ34 peptide sequences.

## Materials and methods

Two single-substitution cysteine mutants, calmodulin-S38C and calmodulin-N111C, were formed by standard methods using the calmodulin construct as previously described (Browne et al. 1997). The proteins were expressed in *Escherichia coli* and purified using phenyl sepharose hydrophobic chromatography as described for wild-type and mutant calmodulins (Browne et al. 1997). The molecular mass of the purified mutants was confirmed by mass spectrometry. Each protein was reacted for 20 min at pH 7 with a three-fold excess of the fluorescent probe Alexa488 maleimide (Molecular Probes, Ore., USA), and the labelled product separated by gel filtration. Synthetic N-Ac and C-amide protected IQ3, IQ4 and IQ34 peptides were purchased from the University of Bristol (UK) and characterized by HPLC, optical spectroscopy and mass spectrometry (Browne et al. 1997; Martin and Bayley 2002).

Fluorescence lifetime and anisotropy measurements were performed by phase-fluorometry (Beechem et al. 1991), using calmodulin with Alexa488 attached to either the N- or C-domain. Excitation was at 450 nm by frequency doubling of the pulse-picked (4 MHz) emission at 900 nm of a Spectra Physics Tsunami Ti:sapphire mode-locked picosecond laser. Emission was observed via a monochromator at 530 nm with 8 nm bandpass, with an ISS multi-frequency fluorimeter operating from 4 to 200 MHz, using fluorescein as a lifetime standard (4.0 ns). Steady-state measurements were also made on an ISS photon-counting fluorimeter.

All spectroscopic measurements were performed at 21 °C in 25 mM Tris (pH 8.0) containing 100 mM KCl and either 1 mM EGTA (for apo-calmodulin) or 1 mM  $\text{Ca}^{2+}$  (for  $\text{Ca}_4\text{calmodulin}$ ), using a calmodulin concentration of 1  $\mu\text{M}$ . The peptide affinity for formation of 1:1 complexes of apo-Cam with either IQ3 or IQ4 was estimated as  $K_d < 20$  nM by fluorescent titrations using the IQ3 peptide Trp emission (Martin and Bayley 2002). A peptide:Cam molar ratio of 1.1 was used to generate the equimolar complexes of IQ3 or IQ4 with apo- and  $\text{Ca}_4\text{Cam}$ .

Data analysis was performed with Globals software (Laboratory of Fluorescence Dynamics, Urbana, Ill., USA). Lifetimes were analysed with one or two components; the data (4–200 MHz) were generally well fitted with a single exponential decay (fractional intensity >95%), with  $\tau = 4.0 \pm 0.1$  ns. Anisotropy analysis used a single  $\tau$  and always required two correlation times,  $\phi_1$  (global rotation) and  $\phi_2$  (<0.3 ns; fast probe rotation), with fractional intensities  $f_1$  and  $f_2$ . The fast motion is interpreted as tumbling in a cone of half-angle  $\theta$ , using  $f_1 = [\frac{1}{2}\cos\theta(1 + \cos\theta)]^2$  (Kinosita et al. 1977). Thus  $\theta \approx 25\text{--}50^\circ$ , for  $0.4 < f_2 < 0.7$ . The value of  $r_0$  was fixed at 0.38, as measured for Cam111A +  $\text{Ca}^{2+}$  at  $-15^\circ\text{C}$  in glycerol (Bayley PM, Anson M, unpublished work). Fitting was by Marquardt algorithm to minimize  $\chi^2$ , and applying rigorous confidence limits such that only individual  $\phi_1$  and  $f_1$  values with limits of  $< \pm 5\%$  were accepted. The standard deviations reported in Table 1 are those for independent measurements on different samples and in different experimental sessions over a period of several days. An increase in either  $\phi_1$  or  $f_1$  indicates a decrease in the rate or increase in the amplitude of the slower motion. The confidence limits on  $\phi_1$  are somewhat larger than desired, due to some correlation between values of  $\phi_1$  and  $f_1$  in the fitting. We also calculate the product,  $Z = f_1 \times \phi_1$ , representing the contribution of the global rotation to the integrated area of the rotational correlation function,  $\{r(t) = \sum f_i r_{i0} \exp(-t/\phi_i)\}$ . The value of  $Z$  can be compared with the calculated value of  $\phi_1$  for purely Brownian rotation of the protein (or complex), taken as an equivalent hydrated sphere, which is 7.2 ns for Cam-IQ3 or Cam-IQ4, and 8.4 ns for Cam-IQ34.

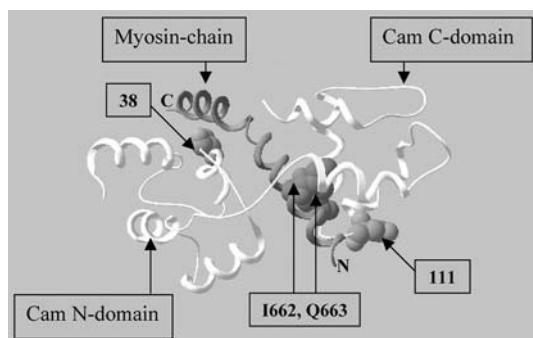


**Fig. 1** Schematic diagram of the structural model of apo-calmodulin (white ribbon) bound to the chicken brush border myosin-I IQ peptide, residues 654–686 (grey ribbon) (1aji.pdb, Houdusse et al. 1996). The IQ residues (spacefilled, I662 and Q663) are seen to be in contact with the C-terminal domain of the apo-calmodulin. Positions 38 and 111 of the two cysteine mutations used in this work are indicated

**Table 1** Time-resolved fluorescence anisotropy of 1:1 calmodulin-IQ peptide complexes, analysed as a two-component system

CamX	Cam38A $\phi_1$ (ns) <sup>a</sup>	Cam38A $f_1$ <sup>b</sup>	$Z_{38}$	Cam111A $\phi_1$ (ns) <sup>a</sup>	Cam111A $f_1$ <sup>b</sup>	$Z_{111}$
Apo-CamX	3.37 ± 0.49	0.36	1.21	3.88 ± 0.29	0.41	1.59
Apo-CamX + IQ3	3.63 ± 0.21	0.37	1.34	5.83 ± 0.01	0.40	2.33
Apo-CamX + IQ4	4.28 ± 0.11	0.33	1.41	5.29 ± 0.5*	0.46	2.43
CamX + Ca <sup>2+</sup>	5.15 ± 0.33	0.52	2.68	5.05 ± 0.09	0.53	2.68
CamX + Ca <sup>2+</sup> + IQ3	6.03 ± 0.40	0.61	3.68	6.63 ± 0.30	0.68	4.51
CamX + Ca <sup>2+</sup> + IQ4	6.83 ± 0.4*	0.55	3.76	7.11 ± 0.30	0.69	4.90
CamX + Ca <sup>2+</sup> + IQ34	8.13 ± 0.30	0.69	5.61	8.42 ± 0.40	0.68	5.72

<sup>a</sup> $\phi_1$  is the slower (global) rotational relaxation time (mean ± s.d.,  $n = 3$ ; \*single value ± confidence limits,  $n = 1$ )

<sup>b</sup> $f_1$  is the fractional amplitude;  $\phi_2$  (< 0.3 ns) reflects fast segmental motion, with cone half-angle from 28° to 47° for  $f_1 = 0.69$ –0.33) (the parameter  $Z = \phi_1 \times f_1$  for each data set; see Materials and methods)

Figure 1 was prepared with Swiss Pdb Viewer [http://www.expasy.ch/spdbv/ (Guex and Peitsch 1997)].

## Results

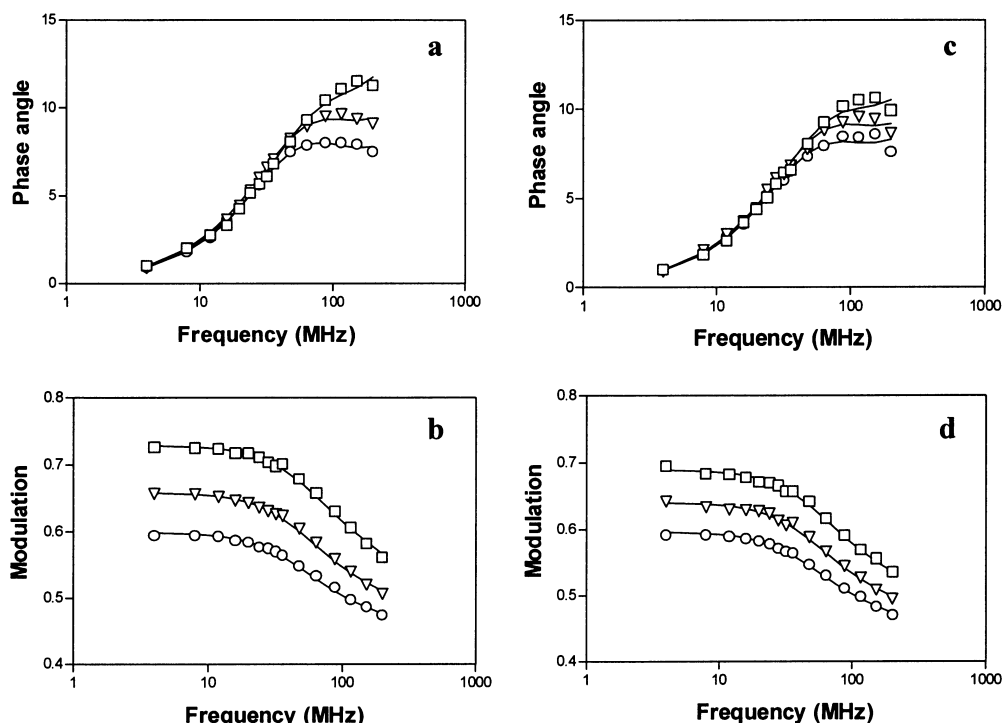
The choice of positions for the attachment of the labels was based on the X-ray and NMR structures of Ca<sub>4</sub>-Cam with skMLCK or smMLCK peptides. Residues 38 and 111 are in homologous positions in the two domains, which are themselves related by gene duplication. These residues are symmetry-related residues on the external surface of the Ca<sub>4</sub>-Cam-skMLCK peptide complex (Barth et al. 1998). Their locations on the proposed structure for the apo-Cam complex with an IQ sequence (laji.pdb; Fig. 1) shows that the two probes should sample potentially significantly different spatial and dynamic environments. Alexa488 has advantages for anisotropy studies of being a photostable fluoro-

phore with high quantum yield and sensitivity. The independence of fluorescence emission maximum and lifetime to experimental conditions makes this fluorophore highly suitable for measuring rotational correlation times of proteins in the range 5–50 kD ( $\phi = 2$ –20 ns).

Typical results of anisotropy measurements are shown in Fig. 2 and Table 1. All measurements of the time-resolved anisotropy show the presence of a fast correlation time  $\phi_2$  (< 0.3 ns), attributed to the independent segmental motion of the fluorescent probe, and a well-resolved major component  $\phi_1$ , corresponding to a more global motion.

The observed value for  $\phi_1$  of < 4 ns for the labelled apo-proteins is significantly faster than the rotational correlation time expected for apo-calmodulin, considered as a spherical globular protein of 16.5 kD molecular mass (~6.6 ns at 25 °C in water). Calmodulin is expected to show complex hydrodynamic properties,

**Fig. 2** Typical experimental traces of differential frequency response curves for holo-Cam38-Alexa488 (**a**, phase; **b**, modulation) and holo-Cam111-Alexa488 (**c**, phase; **d**, modulation) for the protein alone (*squares*), in the presence of the IQ3 peptide (*triangles*) and in the presence of IQ34 peptide (*circles*). The *lines* show fitted functions. See Materials and methods section for data collection and analysis



given its two-domain structure, with limited contact between the domains in both the presence and absence of  $\text{Ca}^{2+}$  (Finn et al. 1995; Kuboniwa et al. 1995; Zhang et al. 1995). For both apo-Cam111A and apo-Cam38A,  $\phi 1$  is close to the value of  $\sim 3.5$  ns calculated for a single spherical domain of mass 8–9 kD, implying motion virtually independent of the other (unlabelled) domain. The rotational mobility of apo-C-domain (C111-labelled) is decreased by peptide IQ3 or IQ4, indicating that the C-domain is the primary site of interaction, consistent with fluorescence and CD studies (Martin and Bayley 2002). By contrast, the values of  $\phi 1$  and  $f1$  for the apo-N-domain (C38-labelled) are significantly less affected by binding either peptide, and remain close to the value for a single domain (studies of complexes of apo-calmodulins + IQ34 were excluded owing to their insolubility).

Binding of  $\text{Ca}^{2+}$  to form either  $\text{Ca}_4\text{Cam38A}$  or  $\text{Ca}_4\text{Cam111A}$  causes an increase in both  $\phi 1$  and  $f1$ , the fraction of the slow global rotational component (which is also indicated by the integrated product,  $Z = f1\phi 1$ ). The values of  $\phi 1$  for  $\text{Ca}_4\text{CaM}$  are still significantly smaller than expected for the global tumbling of the whole molecule. Larger values have been reported from NMR relaxation measurements, albeit at significantly higher concentration [1.5 mM  $\text{Ca}_4\text{calmodulin}$  at pH 6.3 (Barbato et al. 1992)]. The  $\text{Ca}^{2+}$ -induced conformational transition changes the relative spatial arrangement of the helices, including the last helix of the N-domain and the first helix of the C-domain (Finn et al. 1995; Kuboniwa et al. 1995; Zhang et al. 1995), although the intervening residues are flexible (Barbato et al. 1992; Persechini and Kretsinger 1988). The results therefore reflect an increase in the effective total hydrodynamic mass.

The hydrodynamic properties of the complex of  $\text{Ca}_4\text{CaM}$  with IQ target peptides show a further marked increase in  $\phi 1$  and  $f1$  for both  $\text{Ca}_4\text{Cam-IQ3}$  and  $\text{Ca}_4\text{Cam-IQ4}$  complexes. IQ3 and IQ4 have quite similar effects with a given labelled calmodulin; complex formation results in similar dynamics of the labelled N-domain of  $\text{Ca}_4\text{Cam38A}$  and the labelled C-domain of  $\text{Ca}_4\text{Cam111A}$ , with  $\phi 1$  in the range 6–7 ns, approaching the rotational correlation time (7.2 ns) calculated for an approximately spherical particle with the total mass of the complex, i.e.  $M_r \approx 18$  kD. The interaction of either labelled  $\text{Ca}_4\text{CaM}$  with the double-length IQ34 peptide shows increased values of  $f1$  (0.68), indicating more restricted probe motion, and values of  $\phi 1$  (8.1–8.4 ns) corresponding to the global rotation of a particle with the total mass ( $\sim 20$ –21 kD) for a  $\text{CaM-IQ34}$  complex with 1:1 stoichiometry. The maximum value of  $Z$  observed for  $\text{CaM-IQ3/IQ4}$  (4.9/7.2) and 1:1  $\text{CaM-IQ34}$  (5.72/8.4) is 68% in both cases. Thus, under these limiting conditions, while either fluorescent probe retains a significant amount (32%) of fast segmental motion, the value of the slow correlation time  $\phi 1$  indicates that rotational coupling of the two domains is effectively complete. Measurements as a function of the

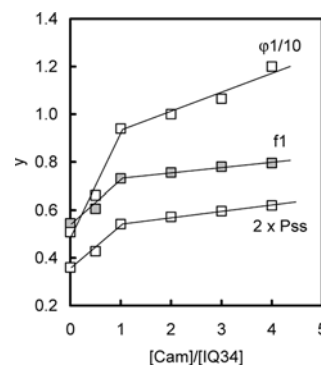


**Fig. 3** Titration of IQ34 (1  $\mu\text{M}$ ) with  $\text{Ca}_4\text{CaM111-Alexa488}$  studied by steady-state fluorescence polarization ( $P_{ss}$ ) and time-resolved fluorescence anisotropy ( $\phi 1$  and  $f1$ ); pH 8, 1 mM  $\text{Ca}^{2+}$ , 25  $^\circ\text{C}$ . Plots of  $P_{ss}$  and  $\phi 1$  have been scaled for comparison with  $f1$

$\text{CaM/IQ34}$  ratio are shown in Fig. 3. All three parameters,  $\phi 1$ ,  $f1$  and  $P_{ss}$  (steady state polarization), are observed to conform to a 1:1 stoichiometry.

## Discussion

Using a single fluorescent probe in homologous positions within two domains of calmodulin, the observed real-time fluorescence anisotropy decay corresponds to a fast process, typical of the independent segmental rotation of the probe, which occurs irrespective of the domain to which it is attached, and with an amplitude corresponding to a cone half-angle of  $\sim 47^\circ$ . This fast process is accompanied by a slower process, corresponding to a more global rotational diffusion of the protein itself. The value of the rotational correlation coefficient increases progressively with the binding of  $\text{Ca}^{2+}$  and peptides as ligands (Table 1). These results show that the rotational dynamic properties of an individual domain can be distinguished from that of the full molecular mass. Effects on these structural dynamics are observed which are specific to either domain in terms of the sensitivity to the apo (Ca-free) versus holo (Ca-bound) state of calmodulin, and also to the binding of the IQ target peptides. In the apo state of calmodulin, both domains show global rotation corresponding to a single domain; however, there is a significant distinction between the dynamic properties of the two domains of apo-calmodulin in the complexes with IQ3 or IQ4 peptide. The C-domain shows decreased motion indicative of a greater effective hydrodynamic mass, whereas the N-domain appears relatively unrestricted in its motion. This result is consistent with the observed dominant effect of the C-domain in the peptide interactions, and the measured low affinity of the isolated apo-N-domain with either IQ peptide (Martin and Bayley 2002). It also shows that the N-domain of calmodulin retains considerable diffusional freedom in the complex involving either IQ-peptide sequence and apo-calmodulin.

By contrast, in addition to the increase in  $\phi 1$  due to the effect of  $\text{Ca}^{2+}$  on calmodulin itself, the results show

that there is a further increase in  $\phi_1$  (and Z1) on formation of the holo complex with either IQ3 or IQ4. These results, reflecting an increase in the effective total hydrodynamic mass, imply an increase in the extent of hydrodynamic coupling of the two domains. For Ca<sub>4</sub>-Cam111A complexes, the value of  $\phi_1 \approx 7$  ns corresponds to a total mass of  $\sim 18$  kD (cf., calculated 18.6 kD). For Ca<sub>4</sub>-Cam-38A complexes, the smaller value of  $\phi_1$  suggests that the labelled N-domain probe may sample a different dynamic environment from C-domain, possibly reflecting the less restrictive constraint on interactions of the closed conformation of this domain, as implied by the structure 1aji.pdb (Fig. 1).

These results are relevant to several aspects of current ideas of the role of Ca<sup>2+</sup> in the regulation of the motor activity of unconventional myosins (reviewed in Geeves 2002). Firstly, the concatenated IQ region is considered to be an integral structural element, stabilized by light chain binding and determining the step size and speed of the motor. The observed weakness of binding and the greater dynamic range of the apo-N-domain is therefore surprising, in view of the projected mechanism of calmodulin action. This involves the general principle of both domains of apo-calmodulin being bound to an individual IQ sequence by both its domains, in order for the 6IQ region to act as a structural element in the “lever-arm” of unconventional myosin I and V. Secondly, the motility of myosin I and V is potentially regulated via the Ca<sup>2+</sup>-induced dissociation of calmodulin (Collins et al. 1990; Homma et al. 2000; Inoue and Ikebe 2001; Zhu et al. 1996, 1998). However, the present results show no evidence for the implied Ca<sup>2+</sup>-induced dissociation of these labelled Cam-IQ target peptide complexes. Similar results were also found for the enhanced affinity of IQ peptides for calmodulin in the presence of Ca<sup>2+</sup> (Martin and Bayley 2002).

Finally, the hydrodynamic properties of Ca<sub>4</sub>-Cam111A and Ca<sub>4</sub>-Cam38A with the double-length IQ34 peptide confirm the equimolar stoichiometry, as observed by direct titration (Fig. 3). The fact that this complex shows hydrodynamic properties consistent with a 20 kD mass indicates that it comprises one molecule each of calmodulin and the IQ34 peptide, and not some multiple thereof, consistent with analytical ultracentrifugation of the complex of wt-Ca<sub>4</sub>-CaM with IQ34 (Martin and Bayley 2002). The observed correlation time indicates a compact structure, supporting the view on purely steric grounds from studies of wt-Cam that it is unlikely that the IQ34 target peptide in such complexes could adopt a continuous  $\alpha$ -helical conformation. However, the continuous helix containing the 6IQ region complexed with apo-calmodulin appears to be a necessary structural requirement to maintain the function of myosin-V (Mehta et al. 1999; Walker et al. 2000). In addition, the fact that the double-length IQ34 peptide (i.e., 2IQ's) binds to a single calmodulin, due principally to the substantial Ca<sup>2+</sup>-dependent increase of the affinity of the calmodulin N-domain for an IQ motif, indicates a lower

stoichiometry (compared to one apo-calmodulin per IQ motif). This would also rationalize why Ca<sup>2+</sup> causes the loss of one (or more) calmodulins from the IQ region of unconventional myosins, as noted above.

On the basis of these results we conclude that, in general, interactions of calmodulin with proteins containing IQ motifs appear likely to comprise a variety of molecular mechanisms as regards their Ca<sup>2+</sup> sensitivity and domain specificity. The results suggest that the properties of the concatenated IQ sequences of unconventional myosins and their attached apo-calmodulin molecules may well include different and complementary contributions from individual IQ sequences. This, together with possible interactions between adjacent calmodulin binding sites, may therefore help to account for the diversity of motility and regulatory properties within this structurally related family of motor proteins.

**Acknowledgements** We are grateful to Dr. Kathy Beckingham, Rice University, USA, for the provision of the original calmodulin construct; Dr. Stephen Howells, NIMR, for mass spectrometry measurements; and Dr. Michael Anson, NIMR, for helpful discussions. We acknowledge support (to P.B. and C.R.) from British Council Alliance Partnership Grant PN 01.047.

## References

- Anderson SR (1991) Time-resolved fluorescence spectroscopy. Applications to calmodulin. *J Biol Chem* 266:11405–11408
- Barbato G, Ikura M, Kay LE, Pastor RW, Bax A (1992) Backbone dynamics of calmodulin studied by <sup>15</sup>N relaxation using inverse detected two-dimensional NMR spectroscopy: the central helix is flexible. *Biochemistry* 31:5269–5278
- Barth A, Martin SR, Bayley PM (1998) Specificity and symmetry in the interaction of calmodulin domains with the skeletal muscle myosin light chain kinase target sequence. *J Biol Chem* 273:2174–2183
- Bayley PM, Martin SR, Jones G (1988) The conformation of calmodulin: a substantial environmentally sensitive helical transition in Ca<sub>4</sub>-calmodulin with potential mechanistic function. *FEBS Lett* 238:61–66
- Bayley PM, Martin SR, Browne JP, Royer CA (2002) Time-resolved anisotropy studies of domain-specific interactions of calmodulin with target sequences of myosin V. *Biophys J* 82:409a
- Beechem JM, Gratton E, Ameloot M, Knutson JR, Brand L (1991) The global analysis of fluorescence intensity and anisotropy data: second generation theory and programs. In: Lakowicz JR (ed) *Topics in fluorescence spectroscopy*, vol 2. Plenum Press, New York, pp 241–305
- Browne JP, Strom M, Martin SR, Bayley PM (1997) The role of  $\beta$ -sheet interactions in domain stability, folding, and target recognition reactions of calmodulin. *Biochemistry* 36:9550–9561
- Collins K, Sellers JR, Matsudaira P (1990) Calmodulin dissociation regulates brush border myosin I (110kD-calmodulin) mechanochemical activity in vitro. *J Cell Biol* 110:1137–1147
- Cope MJ, Whisstock J, Rayment I, Kendrick-Jones J (1996) Conservation within the myosin motor domain: implications for structure and function. *Structure* 4:969–987
- Crivici A, Ikura M (1995) Molecular and structural basis of target recognition by calmodulin. *Annu Rev Biophys Biomol Struct* 24:85–116
- De La Cruz EM, Wells AL, Sweeney HL, Ostap EM (2000) Actin and light chain isoform dependence of myosin V kinetics. *Biochemistry* 39:14196–14202

- Finn BE, Evenäs J, Drakenberg T, Waltho JP, Thulin E, Forsén S (1995) Calcium-induced structural changes and domain autonomy in calmodulin. *Nat Struct Biol* 2:777–783
- Geeves MA (2002) Stretching the lever-arm theory. *Nature* 415:129–130
- Guex N, Peitsch MC (1997) SWISS-MODEL and the Swiss-Pdb-Viewer: an environment for comparative protein modeling. *Electrophoresis* 18:2714–2723
- Homma K, Saito J, Ikebe R, Ikebe M (2000)  $\text{Ca}^{2+}$ -dependent regulation of the motor activity of myosin V. *J Biol Chem* 275:34766–34771
- Houdusse A, Cohen C (1996) Structure of the regulatory domain of scallop myosin at 2 Å resolution: implications for regulation. *Structure* 4:21–32
- Houdusse A, Silver M, Cohen C (1996) A model of  $\text{Ca}^{2+}$ -free calmodulin binding to unconventional myosins reveals how calmodulin acts as a regulatory switch. *Structure* 4:1475–1490
- Houdusse A, Gaucher J-F, Mui S, Kremntsova E, Trybus KM, Cohen C (2000) Crystal structure of calmodulin bound to the IQ motifs of myosin V. *Biophys J* 78:272A
- Inoue A, Ikebe M (2001) Role of the IQ motifs on the regulation of motor activities of myosin I $\beta$ . *Mol Biol Cell* 12:1606
- Kinosita K Jr, Kawato S, Ikegami A (1977) A theory of fluorescence polarization decay in membranes. *Biophys J* 20:289–305
- Kuboniwa H, Tjandra N, Grzesiek S, Ren H, Klee CB, Bax A (1995) Solution structure of calcium-free calmodulin. *Nat Struct Biol* 2:768–776
- Martin SR, Bayley PM (2002) Regulatory implications of a novel mode of interaction of calmodulin with a double IQ motif target sequence from murine dilute myosin V. *Protein Sci* 11:2909–2923
- Mehta AD, Rock RS, Rief M, Spudich JA, Mooseker MS, Cheney RE (1999) Myosin-V is a processive actin-based motor. *Nature* 400:590–593
- Persechini A, Kretsinger RH (1988) The central helix of calmodulin functions as a flexible tether. *J Biol Chem* 263:12175–12178
- Swindells MB, Ikura M (1996) Pre-formation of the semi-open conformation by the apo-calmodulin C-terminal domain and implications for binding IQ-motifs. *Nat Struct Biol* 3:501–504
- Török K, Lane AN, Martin SR, Janot JM, Bayley PM (1992) Effects of calcium binding on the internal dynamic properties of bovine brain calmodulin, studied by NMR and optical spectroscopy. *Biochemistry* 31:3452–3462
- Walker ML, Burgess SA, Sellers JR, Wang F, Hammer JA III, Trinick J, Knight PJ (2000) Two-headed binding of a processive myosin to F-actin. *Nature* 405:804–807
- Wang F, Chen L, Arcucci O, Harvey EV, Bowers B, Xu Y, Hammer JA III, Sellers JR (2000) Effect of ADP and ionic strength on the kinetic and motile properties of recombinant mouse myosin V. *J Biol Chem* 275:4329–4335
- Zhang M, Tanaka T, Ikura M (1995) Calcium-induced conformational transition revealed by the solution structure of apo calmodulin. *Nat Struct Biol* 2:758–767
- Zhu T, Sata M, Ikebe M (1996) Functional expression of mammalian myosin I $\beta$ : analysis of its motor activity. *Biochemistry* 35:513–522
- Zhu T, Beckingham K, Ikebe M (1998) High affinity  $\text{Ca}^{2+}$  binding sites of calmodulin are critical for the regulation of myosin I $\beta$  motor function. *J Biol Chem* 273:20481–20486